

Supermodes for optical transmission

Cen Xia,^{1,*} Neng Bai,¹ Ibrahim Ozdur,¹ Xiang Zhou² and Guifang Li¹

¹CREOL: The College of Optics and Photonics, Univ. of Central Florida, Orlando, FL, 32826 USA

²AT&T Labs-Research, 200 Laurel Ave South, Middletown, NJ, 07748, USA

*cxia@creol.ucf.edu

Abstract: In this paper, the concept of supermode is introduced for long-distance optical transmission systems. The supermodes exploit coupling between the cores of a multi-core fiber, in which the core-to-core distance is much shorter than that in conventional multi-core fiber. The use of supermodes leads to a larger mode effective area and higher mode density than the conventional multi-core fiber. Through simulations, we show that the proposed coupled multi-core fiber allows lower modal dependent loss, mode coupling and differential modal group delay than few-mode fibers. These properties suggest that the coupled multi-core fiber could be a good candidate for both spatial division multiplexing and single-mode operation.

©2011 Optical Society of America

OCIS codes: (060.2280) Fiber design and fabrication; (060.4005) Microstructured fibers; (060.2310) Fiber optics; (060.2330) Fiber optics communications.

References and links

1. P. P. Mitra and J. B. Stark, "Nonlinear limits to the information capacity of optical fibre communications," *Nature* **411**(6841), 1027–1030 (2001).
 2. F. Yaman, N. Bai, B. Zhu, T. Wang, and G. Li, "Long distance transmission in few-mode fibers," *Opt. Express* **18**(12), 13250–13257 (2010), <http://www.opticsinfobase.org/abstract.cfm?URI=oe-18-12-13250>.
 3. B. Zhu, T. Thierry, F. Michael, X. Liu, C. Sethumadhavan, Y. Man, F. John, M. Eric, and D. Frank, "Space-, Wavelength-, Polarization-Division Multiplexed Transmission of 56-Tb/s over a 76.8-km Seven-Core Fiber," in *Optical Fiber Communication Conference* (Optical Society of America, 2011), p. PDPB7.
 4. S. Jun, A. Yoshinari, W. Naoya, K. Atsushi, K. Tetsuya, H. Tetsuya, T. Toshiaki, K. Tetsuya, and W. Masayuki, "109-Tb/s (7x97x172-Gb/s SDM/WDM/PDM) QPSK transmission through 16.8-km homogeneous multi-core fiber," in *National Fiber Optic Engineers Conference* (Optical Society of America, 2011), p. PDPB6.
 5. L. An, A. Abdullah Al, C. Xi, and S. William, "Reception of Mode and Polarization Multiplexed 107-Gb/s CO-OFDM Signal over a Two-Mode Fiber," in *Optical Fiber Communication Conference* (Optical Society of America, 2011), p. PDPB8.
 6. S. Massimiliano, K. Clemens, S. Donato, T. Patrice, B. Patrick, M. Haik, B. Sébastien, B. Aurélien, V. Frederic, S. Pierre, B.-A. Marianne, P. Lionel, C. Frederic, and C. Gabriel, "Transmission at 2x100Gb/s, over Two Modes of 40km-long Prototype Few-Mode Fiber, using LCOS based Mode Multiplexer and Demultiplexer," in *National Fiber Optic Engineers Conference* (Optical Society of America, 2011), p. PDPB9.
 7. R. Roland, R. Sebastian, H. G. Alan, B. Cristian, E. Rene-Jean, W. Peter, W. P. David, M. Alan, and L. Robert, "Space-division multiplexing over 10 km of three-mode fiber using coherent 6 x 6 MIMO processing," in *Optical Fiber Communication Conference* (Optical Society of America, 2011), p. PDPB10.
 8. H. Tetsuya, T. Toshiaki, S. Osamu, S. Takashi, and S. Eisuke, "Ultra-Low-Crosstalk Multi-Core Fiber Feasible to Ultra-Long-Haul Transmission," in *Optical Fiber Communication Conference* (Optical Society of America, 2011), p. PDPC2.
 9. Y. Kokubun and M. Koshiba, "Novel multi-core fibers for mode division multiplexing: proposal and design principle," *IEICE Electron. Express* **6**(8), 522–528 (2009).
 10. N. Kishi and E. Yamashita, "A simple coupled-mode analysis method for multiple-core optical fiber and coupled dielectric waveguide structures," *IEEE Trans. Micro. Theory Techn.* **36**(12), 1861–1868 (1988).
 11. W. Snyder, "Coupled-mode theory for optical fibers," *J. Opt. Soc. Am.* **62**(11), 1267–1277 (1972).
 12. G. P. Agrawal, *Nonlinear fiber optics* (Academic Press 1995).
 13. D. Marcuse, "Curvature loss formula for optical fibers," *J. Opt. Soc. A* **66**(3), 216–220 (1976).
 14. P. M. Krummrich and K. Petermann, "Evaluation of Potential Optical Amplifier Concepts for Coherent Mode Multiplexing" *Proc. OFC 2011, Paper OMH5, Los Angeles, CA, USA* (2011)
 15. H. Kubota, H. Takara, T. Nakagawa, M. Matsui, and T. Morioka, "Intermodal group velocity dispersion of few-mode fiber," *IEICE Electron. Express* **7**(20), 1552–1556 (2010).
-

1. Introduction

Capacity limits for single-mode fiber transmission has been the subject of research for many years since it was recognized that the Kerr nonlinearity in fiber imposes a fundamental limit on fiber capacity [1]. It is well-known that the nonlinear coefficient is inversely proportional to the effective area in a single-mode fiber. Therefore, a simple and effective way to reduce nonlinear penalty is to increase the fiber core diameter and thus enlarge the effective area. However, this approach is limited by the increased macro-bending loss and/or dispersion. Recently a new method was proposed to increase the core diameter without changing the loss and dispersion properties by using few-mode fibers in single-mode operation [2]. Few-mode fibers (FMF) are defined as optical fibers that support more than one spatial mode but fewer spatial modes than conventional multi-mode fibers. Although FMFs can carry more than one mode, the fundamental mode can be excited and transmitted without mode coupling over very long distances as long as the effective indexes of the supported modes are sufficiently different from each other.

Recently, space-division multiplexing (SDM) has been proposed to increase the fiber capacity. So far several approaches have been reported for SDM, including fiber bundle, multi-core fiber (MCF) [3, 4] and FMF [5–7]. Among these options, fiber bundle is the most straightforward one and still attractive for its simplicity and compatibility. FMF is also a candidate for SDM since it supports a few large-effective-area modes and mode coupling can be avoided if a large effective index difference (ΔN_{eff}) exists among the modes. However, there are some limitations for long-distance SDM using FMFs. First is the large differential modal group delay (DMGD) among the modes. Second is the difference in modal loss, which increases with mode order. In addition, mode coupling is inevitable as the number of modes increases since large effective index difference is hard to maintain for all modes. On the other hand, MCF has been proposed as a strong candidate for SDM due to zero DMGD, equal loss and ultra-low crosstalk between modes [8]. Nevertheless, the mode density of MCFs is quite low in order to maintain low crosstalk. In addition, each mode of an MCF still suffers large nonlinear penalty because its effective area is the same as or smaller than that of an SMF. To balance the trade-off between high mode density and low crosstalk, Y. Kokubun and M. Koshiba investigated coupled modes where identical cores are closely arranged [9]. But the mode density did not improve much because the coupled cores form a linear array.

In this paper, we introduce the coupled multi-core fiber (CMCF) structure with strong core-to-core coupling. Coupling between cores can be manipulated to achieve better transmission properties for coupled modes. Because field distribution of a coupled mode can be seen as a superposition of isolated modes, the coupled modes are also called supermodes. For this reason, supermodes generally have much larger effective area. Due to the unique properties of supermodes, CMCFs can support larger mode effective areas and higher mode densities than the conventional multi-core fiber. In addition, these CMCFs can also have lower modal dependent loss, mode coupling and differential modal group delay than the few-mode fiber. These advantages enable this new type of fiber as a potential candidate for applications of both spatial division multiplexing and single-mode operation.

This paper is organized as follows. Section 2 introduces the basic properties of supermodes by analyzing a four-core CMCF structure. Section 3 demonstrates CMCF designs for single-mode operation and space-division multiplexing including performance comparison between CMCFs and FMFs. Section 4 contains a discussion of the possible candidates of next generation transmission fibers, including CMCFs, conventional MCFs and FMFs. Finally, Section 5 presents the conclusion and future work.

2. Theory

In this section, we present the basic supermode analysis of CMCFs. A four-core CMCF structure, shown in Fig. 1, is selected as an example. Fiber cores are assumed to be identical and each of them supports only one mode. The radius of the cores is r , and the distances between adjacent cores and non-adjacent cores are d_1 and d_2 , respectively. The cores and the

cladding have refractive indices of n_1 and n_2 , respectively. The mode of each isolated core has the same normalized frequency (V-number) $V = \frac{2\pi}{\lambda_0} r \sqrt{n_1^2 - n_2^2}$.

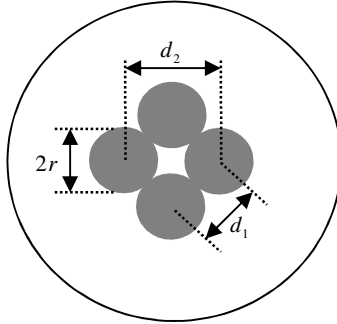


Fig. 1. Schematic of a coupled four-core fiber structure.

According to the coupled-mode analysis [10], the interaction between the modes of the four individual cores can be described by the following coupled-mode equation

$$\frac{d}{dz} \mathbf{A} = -j \overline{\mathbf{M}} \mathbf{A}, \quad (1)$$

where $\mathbf{A} = [A_1 \ A_2 \ A_3 \ A_4]^T$, $\overline{\mathbf{M}} = \begin{pmatrix} \beta_0 & c_1 & c_2 & c_1 \\ c_1 & \beta_0 & c_1 & c_2 \\ c_2 & c_1 & \beta_0 & c_1 \\ c_1 & c_2 & c_1 & \beta_0 \end{pmatrix}$, A_i ($i = 1, 2, 3, 4$) refers to the

complex amplitude of the electrical field of the i^{th} core, β_0 is the propagation constant of the single mode, c_1 and c_2 are the coupling coefficients between adjacent and non-adjacent cores, respectively. Since $\overline{\mathbf{M}}$ is Hermitian for a lossless system, it can be diagonalized by a unitary matrix such that

$$\mathbf{Q}^{-1} \overline{\mathbf{M}} \mathbf{Q} = \mathbf{A}, \quad (2)$$

where \mathbf{A} is a diagonal matrix,

$$\mathbf{A} = \begin{pmatrix} \beta_1 & 0 & 0 & 0 \\ 0 & \beta_2 & 0 & 0 \\ 0 & 0 & \beta_3 & 0 \\ 0 & 0 & 0 & \beta_4 \end{pmatrix} \quad (3)$$

in which β_m ($m = 1, 2, 3, 4$) is the propagation constant of the m^{th} supermode supported by the CMCF. The amplitude matrix for the supermodes is represented as

$$\mathbf{B} = \mathbf{Q}^{-1} \mathbf{A} \quad (4)$$

Under which the coupled-mode Eq. (1) reduces to

$$\frac{d}{dz} \mathbf{B} = -j \mathbf{A} \mathbf{B}. \quad (5)$$

Under the weakly guiding approximation, a general expression of the coupling coefficient c_j ($j = 1, 2$) is given as [11]

$$c_j = \sqrt{\frac{n_1^2 - n_2^2}{n_1^2}} \cdot \frac{1}{r} \cdot \frac{U^2}{V^3} \cdot \frac{K_0(Wd_j/r)}{K_1^2(W)} \quad (6)$$

Where U and W can be found by solving equation $U \cdot K_0(W) \cdot J_1(U) = W \cdot K_1(W) \cdot J_0(U)$ and $U^2 + W^2 = V^2$. The J 's and the K 's are Bessel functions of the first kind and modified Bessel functions of the second kind. After obtaining the coupling coefficients c_1 and c_2 , the supermodes can be solved as eigen-modes. The propagation constant of the supermodes are the eigenvalues, given by:

$$\beta_1 = \beta_0 + 2c_1 + c_2; \beta_2 = \beta_0 - c_2; \beta_3 = \beta_0 - c_2; \beta_4 = \beta_0 - 2c_1 + c_2. \quad (7)$$

The second and third supermodes are degenerate, having the same propagation constants. Using $n_1 = 1.47$, $n_2 = 1.468$, $r = 7 \mu\text{m}$, $d = 14 \mu\text{m}$ and $\lambda = 1.55 \mu\text{m}$, the field distributions of each supermode is calculated and shown in Fig. 2.

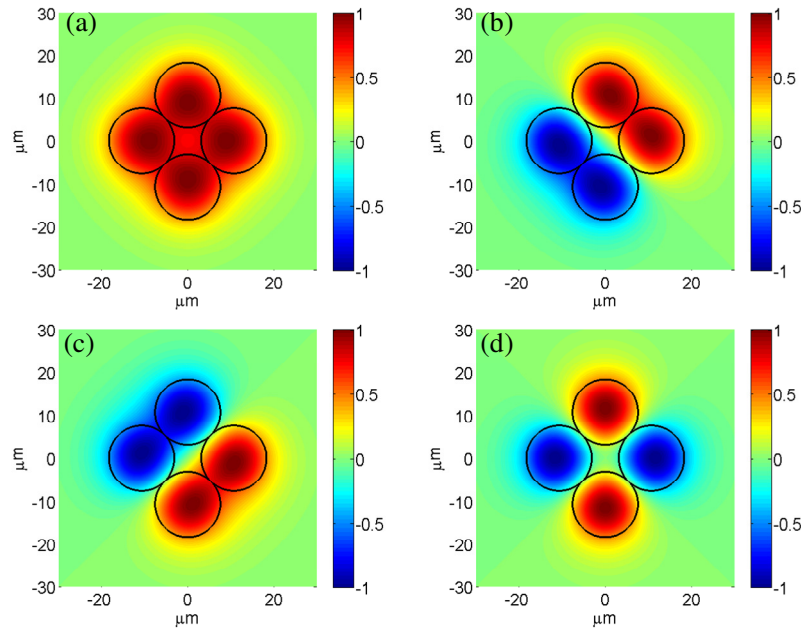


Fig. 2. Field distributions of the 1st (a), 2nd (b), 3rd (c) and 4th (d) supermodes for four-core CMCFs. (Black lines indicate the boundaries of the cores)

One important characteristic of supermodes in four-core CMCFs is that they are superpositions of isolated modes with equal amplitude but not always the same phase. As shown in Fig. 2 (a), the fundamental supermode is the in-phase mode with the largest propagation constant. The higher-order supermodes have the field reversals between adjacent or non-adjacent core regions, shown in Fig. 2(b)-(d). This equal-amplitude characteristic gives similar confinement factors for the supermodes, leading to very small modal dependent loss. It is clear from this example that the properties of supermodes are determined not only by the parameters of each cores but the pitch between cores. In other words, CMCFs have more degrees of freedom or large design space than MCFs and FMFs.

3. Fiber design and application

In this section, CMCFs are designed and applied to both single-mode operation and mode-division-multiplexing applications. For each case, a specific design of CMCF will be presented and compared to FMF in terms of transmission performance.

3.1 CMCF design for single-mode operation

In order to achieve better performance, i.e., reduced nonlinear penalty, in the single-mode operation, the fundamental supermode should have a large effective area A_{eff} given by [12]

$$A_{eff} = \frac{\left| \int_{-\infty}^{+\infty} \int_{-\infty}^{+\infty} I(x, y) dx dy \right|^2}{\int_{-\infty}^{+\infty} \int_{-\infty}^{+\infty} I^2(x, y) dx dy} \quad (8)$$

where $I(x, y)$ is the mode intensity distribution. To minimize mode coupling and guarantee single-mode operation, the fundamental supermode should also have a large difference in effective index ΔN_{eff} , which is given by

$$\Delta N_{eff}(i, j) = \frac{1}{k_0} \cdot (\beta_i - \beta_j) = \frac{1}{k_0} \cdot \sum_n (a_n^i - a_n^j) \cdot c_n \quad (9)$$

Where i and j represent the supermode number, a_n^i and a_n^j denote the coefficient of the coupling coefficient c_n in the expression of β for the i^{th} and j^{th} supermode respectively (see Eq. (7) as an example). The number of modes and the bending loss of the large-area fundamental supermode are two of the most important fiber properties. To make a fair comparison between the CMCFs and FMFs, the macro-bending loss is fixed at 0.0308 dB/m at a mandrel radius of 20 mm and the number of modes is selected to be 6 for both types of fibers. The bending loss value is calculated using the curvature loss formula given by [13] and its value is set in accordance with that for standard SMF fibers. Note that this value represents the minimum bending loss as other factors including micro-bending loss and manufacture imperfection are not included. Both the six-core CMCF and the six-mode fiber have two pair of degenerate modes and two non-degenerate modes. The cores of the 6-core CMCF are arranged to optimize A_{eff} of the fundamental supermode. The fundamental supermode field distribution as well as the core arrangement is shown in Fig. 3(b). In this paper, all designs are based on step-index profiles. As a result, the design variables include the index difference Δ and the core radius r for both CMCFs and FMFs, and an extra parameter, namely, the pitch-to-core ratio (d/r) for CMCFs in addition to the core arrangement.

Before presenting the detailed the comparison, it is worthwhile to have a look at the relationship between the pitch-to-core ratio (d/r) and ΔN_{eff} in CMCFs. From Eq. (6) and (9), it can be seen that a reduced d/r value would increase the coupling coefficient c , and result in a large ΔN_{eff} . Figure 3(a) shows the dependence of A_{eff} and ΔN_{eff} on d/r . As cores are arranged closer, increased coupling between the cores induces a larger split of the effective indexes of supermodes. It is observed that A_{eff} has a weak dependence on d/r while ΔN_{eff} changes sharply with d/r . Therefore the smallest value of d/r ($d/r=2$) is chosen for this comparison.

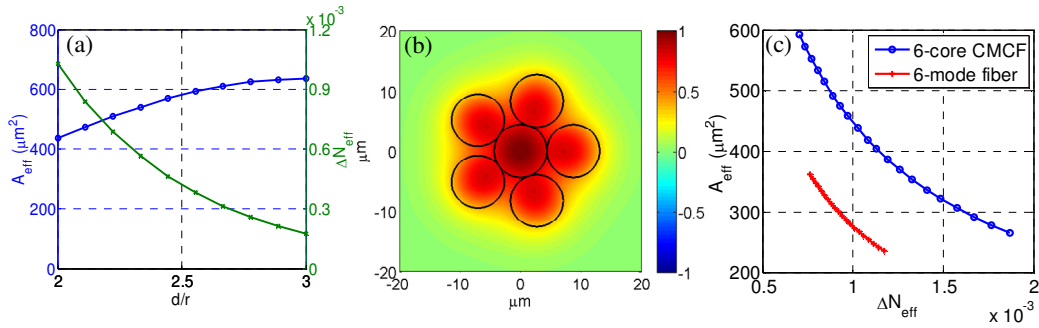


Fig. 3. (a) A_{eff} and ΔN_{eff} vs. d/r for the fundamental mode of six-core CMCFs, (b) the field distribution of the fundamental mode in CMCF (black lines are the boundaries of cores) and (c) A_{eff} vs. ΔN_{eff} for six-core CMCFs and six-mode FMFs.

The fundamental mode properties for the six-core CMCFs and six-mode fibers with the same macro-bending loss are given in Fig. 3(c). It shows that CMCFs perform better in terms of both A_{eff} and ΔN_{eff} . The most important reason for the larger A_{eff} with CMCFs is that, the fundamental supermode is the in-phase superposition of modes of six isolated cores. The larger ΔN_{eff} is mainly attributed to the optimization of extra design freedom d/r . To give a more comprehensive and detailed comparison, ΔN_{eff} is set at a sufficiently large value $1e-3$ for both fibers while other important fiber parameters are listed in Table 1. The A_{eff} of the CMCF is increased by 60% without compromising other properties. Note that slight different index differences (Δ s) are applied to CMCFs and FMFs in order to maintain the same number of modes for both fibers.

Table 1. Properties of Coupled Multi-Core Fiber and Few-Mode Fiber Design for Single-Mode Operation

@ 1.55um	Step-index CMCF	Step-index FMF
Mode number	6	6
Index difference	0.34%	0.23%
Core area (μm^2)	357*	357
Confinement factor	95.8%	95.2%
ΔN_{eff}	$1e-3$	$1e-3$
A_{eff} (μm^2)	438	274
Bending loss 20mm ϕ (dB/m)	0.0308	0.0308
Dispersion (ps/nm/km)	19.2	22.7
Dispersion slope (ps/nm ² /km)	0.077	0.064

*Sum of six single core areas

3.2 CMCF design for space-division multiplexing

It is expected that space-division-multiplexed (SDM) optical transmission can operate successfully either without mode coupling [6] or with mode coupling but with negligible or small differential modal group delay (DMGD) [7]. For the case that there is no mode coupling, modes propagate independently and therefore can be separately detected. For the case with mode coupling but small DMGD, modes may couple to each other, but they can be detected together and then separated by using multiple-input-multiple-output (MIMO) based

digital signal processing (DSP) technique [6, 7]. These two methods can be combined in supermode multiplexing as will be explained below.

In this simulation, the number of mode is selected to be 6 again. However, the core arrangement is without a center core so higher-order supermodes and the fundamental supermode are more symmetrical. The field distributions of the supermodes are shown in Fig. 4. Again, both six-core CMCFs and six-mode fibers support six modes including two pair of degenerate modes and two other non-degenerate modes. For six-mode fibers, the two pairs of degenerate modes are the degenerate LP_{11} and LP_{21} modes. For CMCFs, the two pairs of degenerate modes are the 2nd and 3rd, 4th and 5th supermodes. The degenerate supermodes have identical effective indexes and thus there is no DMGD between them. The non-degenerate supermodes have different effective indexes. Fortunately, these non-degenerate supermodes/supermode groups can be designed to have low crosstalk by maintaining a large ΔN_{eff} between them. Therefore demultiplexing in SDM using CMCFs can be successfully performed in two steps: i) the non-degenerate supermodes/supermode groups are separately detected while the degenerate supermodes are still mixed together; ii) mixed signals in the degenerate supermodes are recovered by the MIMO-based DSP techniques [6, 7].

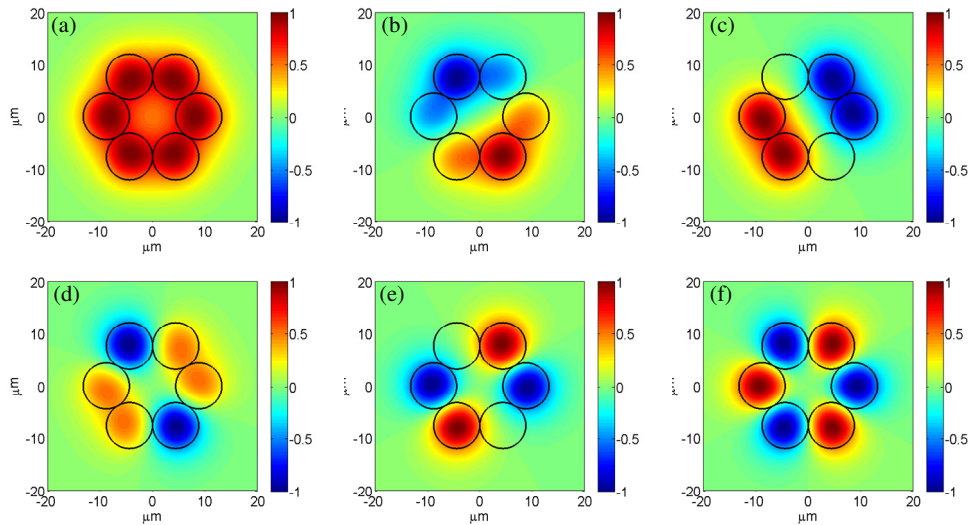


Fig. 4. Field distributions of the 1st (a), 2nd (b), 3rd (c), 4th (d), 5th (e) and 6th (f) supermodes for the six-core CMCF. (Black lines indicate the boundaries of the cores)

There are three design goals to optimize the performance for SDM: (1) ΔN_{eff} between any two modes should be sufficiently large to avoid mode coupling; (2) mode losses need to be similar to each other and as low as possible; (3) large effective areas are always required for reducing nonlinearity. Based on these goals, 6-core CMCFs and 6-mode fibers are designed respectively and their performances are shown in Fig. 5(a) and (b). The macro-bending losses of the fundamental modes for both fibers are fixed at 0.0308 dB/m at a mandrel radius of 20mm. Confinement factor is used here to characterize the mode loss. Higher confinement factor implies lower loss as it indicates less bending loss. From Fig. 5(a) and (b), one can see that CMCFs show a significant advantage of attaining large and similar ΔN_{eff} , confinement and A_{eff} for all supermodes. In other words, the supermodes tend to preserve less mode coupling, lower loss and lower nonlinearity than regular modes. All supermodes have similar properties (including mode coupling, loss and nonlinearity), which is crucial for long-distance mode-division-multiplexing. Higher-order modes in FMF seem to have larger effective areas

in Fig. 5(a), but these large effective areas actually result from low confinement (as indicated in Fig. 5(b)) and hence has no practical benefit.

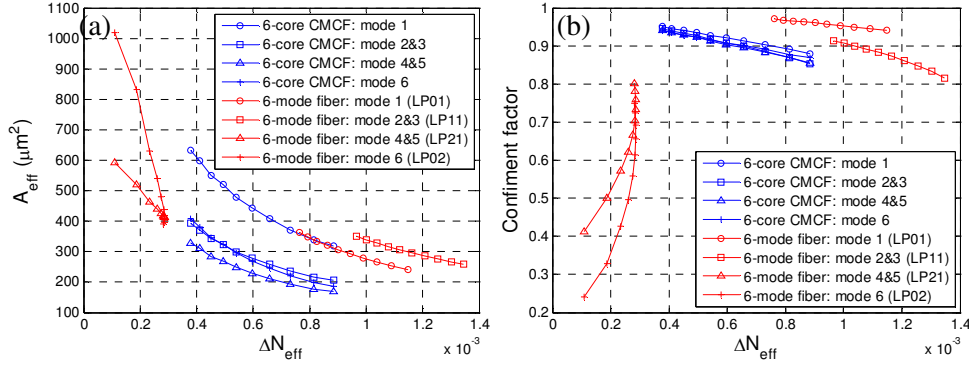


Fig. 5. (a) A_{eff} vs. ΔN_{eff} for CMCFs and FMFs (ΔN_{eff} refers to the minimum ΔN_{eff} for one mode to any other mode). (b) Confinement factor vs. ΔN_{eff} for CMCFs and FMFs

A CMCF design with zero or small DMGD between supermodes has also been considered. In this case, even though supermode coupling may still exist, they travel at the same/similar group velocities. Therefore the supermodes could be detected together and demultiplexing can be performed using MIMO DSP techniques as we mentioned above. According to Eq. (6), DMGD between the i^{th} and j^{th} supermodes, can be represented as

$$\text{DMGD}(i,j) = \frac{d\beta_i}{d\omega} - \frac{d\beta_j}{d\omega} = \sum_{n=1}^2 (a_n^i - a_n^j) \cdot \frac{dc_n}{d\omega} \quad (10)$$

where a_n^i and a_n^j relate the supermode propagation constant β for the i^{th} and j^{th} supermode, respectively, to the coupling coefficients c_n as given in Eq. (7). Using Eq. (6), $\frac{dc_n}{d\omega}$ ($n=1,2$) is obtained as,

$$\frac{dc_n}{d\omega} = \frac{1}{r} \cdot \left\{ \frac{\partial}{\partial \omega} \sqrt{1 - \frac{n_2^2(\omega)}{n_1^2(\omega)}} \cdot \left[\frac{U^2}{V^3} \cdot \frac{K_0(Wd_n/r)}{K_1^2(W)} \right] + \sqrt{1 - \frac{n_2^2}{n_1^2}} \cdot \frac{\partial}{\partial \omega} \left[\frac{U(\omega)^2}{V(\omega)^3} \cdot \frac{K_0(W(\omega) \cdot d_n/r)}{K_1^2(\omega)} \right] \right\} \quad (11)$$

It should be noted that Eq. (10) is presented for four-core CMCFs, in which DMGD is a linear combination of $\frac{dc_1}{d\omega}$ and $\frac{dc_2}{d\omega}$ with different weighting coefficients for different supermodes. It is clear that in order to achieve zero DMGD among all the supermodes, both $\frac{dc_1}{d\omega}$ and $\frac{dc_2}{d\omega}$ should vanish, which is unlikely if not impossible to realize in a simple step-index profile CMCF. This problem also exists for other CMCF structures where the number of cores is more than three. Therefore three-core CMCFs are chosen here for zero DMGD design as they only contain adjacent core coupling, i.e., only one value of c exists. As a result, total DMGD scales with $\frac{dc_1}{d\omega}$, and it is equivalent to attain zero for $\frac{dc_1}{d\omega}$ in order to achieve zero DMGD in this structure. The mode fields of three-core CMCFs are given in Fig. 7, (b), (c) and (d). As shown in Eq. (11), $\frac{dc}{d\omega}$ consists of two parts: a frequency dependent index

(n_1, n_2) component and a frequency dependent waveguide parameters (V, U, W) component, i.e., the material and waveguide DMGD. At the first glance, one might think that material DMGD is larger than waveguide DMGD (material dispersion is dominant in chromatic dispersion of standard SMFs). However, it is incorrect to draw an analogy between DMGD and chromatic dispersion because the nature of DMGD is differential group delay (DGD) between modes instead of dispersion within one mode. In fact, all supermodes propagate in the same material but with different propagation constants, implies that the material DMGD should be negligible compared to waveguide DMGD. This conclusion is verified by simulation. Since material DMGD is significantly smaller than waveguide DMGD, they will be neglected in the following discussion to simplify the analysis.

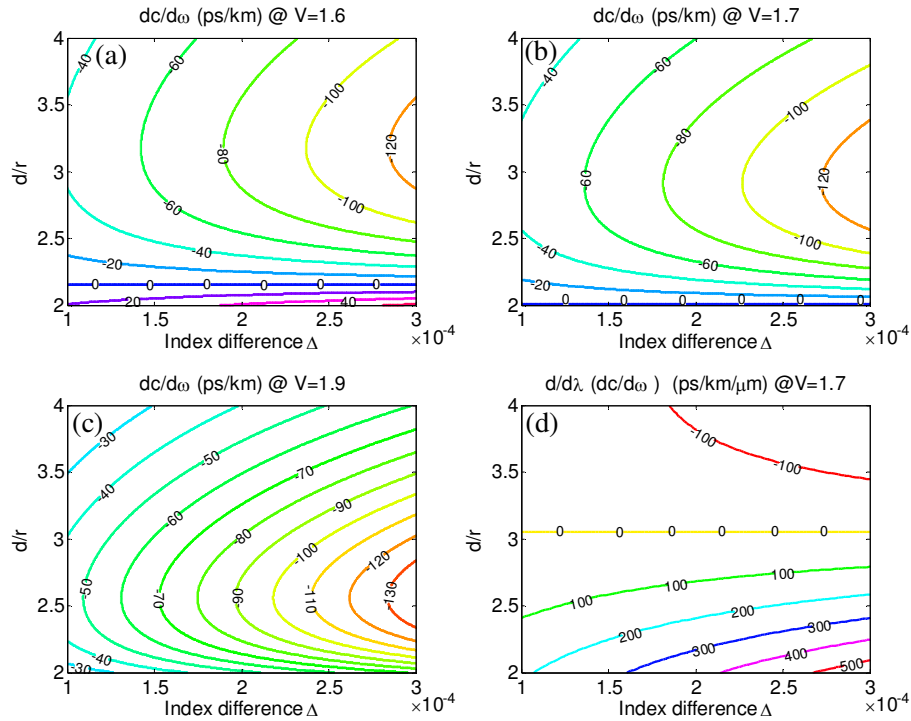


Fig. 6. (a) (b) (c) $\frac{dc}{d\omega}$ at $V=1.6, 1.7$ and 1.9 . (d) $\frac{d}{d\lambda}\left(\frac{dc}{d\omega}\right)$ at $V=1.7$.

As indicated in Eq. (11), $\frac{dc}{d\omega}$ is determined by the pitch-to-core ratio (d/r) , V number and

core radius r (or equivalently, V number and index difference Δ since $V = \frac{2\pi}{\lambda_0} r \sqrt{n_1^2 - n_2^2}$).

Their relationship is shown in Fig. 6(a), (b) and (c). It is confirmed by both analysis and simulation that when the V -number is fixed, zero DMGD is attained if and only if d/r reaches a certain value. As the V -number increases, zero DMGD is realized for a smaller value of d/r , as indicated in Fig. 6(a), (b) and (c). So in order to attain zero DMGD, V -number is limited to below 1.71 because d/r cannot less than 2. This is demonstrated by the zero DMGD horizontal lines and their locations with different V -numbers in Fig. 6(a), (b) and (c) [in Fig. 6(c), with V -number > 1.71 , the zero DMGD line does not exist]. Apart from zero DMGD, a sufficiently small DMGD is enough for practical use as well. This can be obtained by reducing index difference Δ .

To meet the practical application requirements in a WDM system, CMCFs further require small DMGD variation within a certain range of wavelength, i.e., a small modal differential group delay slope (DMGDS). (DMGDS can be regarded as linear within a narrow range of wavelength). Similar to DMGD, DMGDS between the i^{th} and j^{th} supermodes in a three-core structure can be represented as

$$DMGDS(i,j) = \frac{d}{d\lambda} \left(\frac{d\beta_i}{d\omega} - \frac{d\beta_j}{d\omega} \right) = (a_{1i} - a_{1j}) \cdot \frac{d}{d\lambda} \left(\frac{dc_1}{d\omega} \right) \quad (12)$$

Given that material DMGD is negligible, the $\frac{d}{d\lambda} \left(\frac{dc}{d\omega} \right)$ term can be further expressed as

$$\frac{d}{d\lambda} \left(\frac{dC}{d\omega} \right) = \frac{1}{r} \cdot \sqrt{1 - \frac{n_2^2}{n_1^2}} \cdot \frac{\partial^2}{\partial \lambda \cdot \partial \omega} \left[\frac{U(\omega)^2}{V(\omega)^3} \cdot \frac{K_0(W(\omega) \cdot d/r)}{K_1^2(W(\omega))} \right] \quad (13)$$

In Fig. 6(d), DMGDS is plotted vs. (d/r) and Δ . Even though zero DMGDS can be realized, they occur at a larger value of d/r with respect to zero DMGD. Therefore, it will be difficult to achieve zero DMGD and DMGDS simultaneously. Even so, DMGDS can still be reduced by decreasing index difference Δ . Wavelength-dependent DMGD as well as mode fields of a specific three-core CMCF design is given in Fig. 7 (a) and (b). The DMGD is below 60 ps/km over the entire C band, which is the same value achieved by three-mode fiber using a depressed cladding index profile [7].

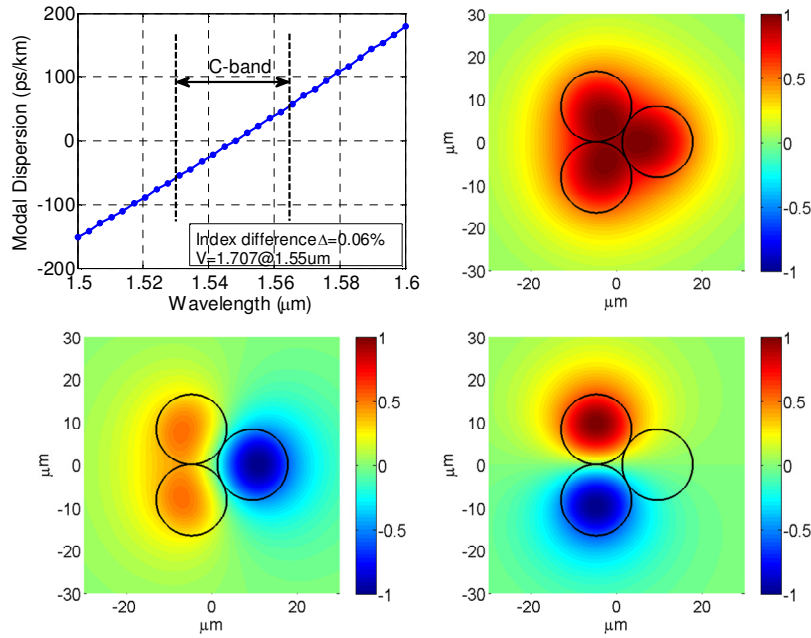


Fig. 7. (a) maximum DMGD vs. wavelength at $V=1.707$ @ $1.55\mu\text{m}$ and $\Delta=0.06\%$, (b) (c) (d) field distribution of the 1st, 2nd and 3rd supermode of a three-core CMCF

4. Discussion

In this section, a comprehensive discussion of the possible candidates of next generation transmission fibers, especially for the application of SDM, is presented. These fibers are MCF, FMF, fiber bundle and the proposed CMCF. Note that even though fiber bundle is usually referred as a bundle of SMFs, it could be a bundle of MCFs, FMFs or CMCFs. In

other words, fiber bundle is only a concept of package form, not a type of fiber. Therefore, only MCF, FMF and CMCF are compared with each other as shown in Table 2.

Table 2. Comparison of Next Generation Transmission Fibers for Spatial Division Multiplexing

	Multi-core fiber (MCF)	Coupled multi-core fiber (CMCF)	Few-mode fiber (FMF)
Transmission property	Spatial Mode Density ^a	Low	High
	Differential Modal Group Delay (DMGD)	Zero	Small (controllable)
	Crosstalk ^b	Low	Easy to Control
	Modal Dependent Loss	Equal	Similar
	Loss	Low	Low
	Effective Area (A_{eff}) ^c	Small	Large
Amplification	Pump coupling	Hard	Easy
	Power efficiency (cladding pump)	Low	High
	Scalability	Good	Good
	Inter-connect	Hard	Hard

^aNumber of spatial modes per unit area of the fiber cross-section

^bCrosstalk between spatial modes (single modes for MCF; supermodes for CMCF; regular modes for FMF)

^cEffective area of spatial modes

The transmission property is the most important part, since it determines the fundamental capacity of the fiber. For SDM transmission, the capacity of the system scales with the number of modes and hence proportional to the spatial mode density. As pointed out before, the spatial mode density of MCFs is much lower than CMCFs and FMFs because of the low crosstalk requirement. Linear crosstalk caused by mode coupling is one of the most critical impairments in both CMCF and FMF system. In order to facilitate spatial demultiplexing and linear crosstalk cancelation, increasing ΔN_{eff} to reduce mode coupling [6] or equalizing DMGD to lessen computation load of MIMO process [7] have to be considered in fiber design. It is shown in this paper that CMCFs have more degrees of design freedom, namely, pitch length and core arrangement and thus improve both ΔN_{eff} and DMGD significantly. Low and equal modal loss is another advantage of CMCFs over FMFs. Similar to MCFs, light is well confined in each core of CMCFs. The confinement factors of all supermodes are relative high and similar. In contrast, high order modes in FMFs have much larger bending loss than the fundamental mode indicated by low confinement factors. In addition, CMCFs can have larger A_{eff} spatial mode than MCFs. Therefore nonlinear impact is directly reduced which leads to higher fundamental capacity of the systems.

For long haul SDM transmission, a low noise and power efficient amplifier is highly required. The design of fiber amplifier should be matched with the type of transmission fiber. In the second part of Table 2, the complexity and performance of amplification are compared among 3 candidate fibers. To reduce amplified stimulated emission noise, most doped ions have to be inverted which requires a pump power scaled with the effective guiding area of the pump [14]. For the case of cladding pump, strong pump is guided in the inner cladding of the active fiber. With a closer spacing between cores, a CMCF amplifier (CMCFA) is expected to have much smaller inner cladding size compared to an MCF amplifier (MCFA). Consequently, the operating pump power can be dramatically reduced. In order to increase power efficiency for MCFAs, pump has to be launched core by core using free space optics [14]. However, the launching scheme requires further alignment complexity.

Another unique property of CMCFs and MCFs is that the number of spatial modes is exactly the same as the core number of the fiber. Any number of spatial modes can be

obtained by adjusting the core number. On the contrary, for FMFs, tuning either core size or index difference cannot always guarantee the desired number of modes and this becomes more problematic as the number of modes grows (For example, FMFs can never support 4 modes including degenerate modes). Lastly, although CMCFs have many improvements compared to other two types of fibers, it shares the same shortage of inter-connection difficulty as MCFs due to a lack of angular symmetry. A slight angular misalignment may lead to a high excess loss. Special devices, similar to polarization maintaining fiber splicers, are necessary for the inter-connection of MCFs and CMCFs [3].

5. Conclusion and future work

We have proposed a coupled multi-core fiber (CMCF) design for long-haul transmission, to the best of our knowledge, for the first time. The new design exploits the coupling between the cores of a conventional multi-core fiber instead of avoiding it. This design has advantageous over the conventional multi-core fiber in terms of higher mode density and larger mode effective area. It is also possible to avoid mode coupling between supermodes through additional degree of design freedom which includes the pitch-to-core ratio and core arrangement. In this paper we focus on four-core, six-core and three-core structures due to their simplicity and symmetry. For the future application, the number and arrangement of the cores can be modified to meet further requirements.

For single-mode operation, CMCFs can attain larger ΔN_{eff} and A_{eff} than FMFs. As a result, they tend to have less mode coupling and nonlinearity, which is vital for efficient long-haul transmission. The excitation of the fundamental supermode (as well as the higher-order supermodes) can be realized using free-space optics which has been used to excite spatial modes of FMFs [6, 7]. In addition, there is a possibility that supermode excitation is even simpler because supermodes can be seen as superpositions of modes of the coupled cores. The crosstalk accumulated in the higher-order supermodes after transmitting certain distance could also be removed optically, by using the phase reversal of higher order supermodes. For example, implementing a 4f-configuration component [6] is able to remove the power of higher-order supermodes in the Fourier plane. It should be noticed that, in this paper we select d/r to be the minimum ($d/r=2$) to optimize both ΔN_{eff} and A_{eff} . In fact, the value of d/r can be tuned to meet a specific individual requirement of a large ΔN_{eff} or A_{eff} .

For mode-division-multiplexing, two concepts can be simultaneously applied in CMCFs. One is to utilize zero DMGD between the two degenerate supermodes and the other is to eliminate mode coupling between the non-degenerate supermodes. Demultiplexing can be realized by first detecting the non-degenerate ones separately and then recover signals mixed in the degenerate supermodes by MIMO DSP techniques. Compared to FMF modes, the supermodes can maintain less mode coupling, nonlinearity and similar loss. The other possibility is to design CMCFs with zero DMGD between all the supermodes and a DMGD slope small enough for WDM system. In this paper, a 60 ps/km DMGD between any two supermodes across the C-band has been demonstrated in a step-index three-core CMCF. This DMGD value can be further reduced by reducing the index difference between the core and cladding. It has been reported that graded-index profiles can decrease DMGD in FMFs [15]. It is likely that a more sophisticated index profile including the graded-index profile for CMCFs may further reduce the DMGD.